AUTOPHAGY
2020, VOL. 16, NO. 6, 1077–1091
https://doi.org/10.1080/15548627.2019.1659610

Taylor & Francis
Taylor & Francis Group

RESEARCH PAPER

LncRNA *2810403D21Rik/Mirf* promotes ischemic myocardial injury by regulating autophagy through targeting *Mir26a*

Haihai Liang[a,b*], Xiaomin Su[a,b*], Qiuxia Wu[a,b], Huitong Shan[a,b], Lifang Lv[a], Tong Yu[a,b], Xiaoguang Zhao[a,b], Jian Sun[a,b], Rui Yang[a], Lu Zhang[a,b], He Yan[a,b], Yuhong Zhou[a], Xuelian Li [a], Zhimin Du[c], and Hongli Shan[a,b]

[a]Department of Pharmacology (State-Province Key Laboratories of Biomedicine-Pharmaceutics of China, Key Laboratory of Cardiovascular Research, Ministry of Education), College of Pharmacy, Harbin Medical University, Harbin, Heilongjiang, P. R. China; [b]Northern Translational Medicine Research and Cooperation Center, Heilongjiang Academy of Medical Sciences, Harbin Medical University, Harbin, Heilongjiang, P. R. China; [c]Institute of Clinical Pharmacy, The 2nd Affiliated Hospital, Harbin Medical University, Harbin, Heilongjiang, P. R. China

ABSTRACT

More evidence is emerging of the roles long non-coding RNAs (lncRNAs) play as regulatory factors in a variety of biological processes, but the mechanisms underlying the function of lncRNAs in acute myocardial infarction (AMI) have not been explicitly delineated. The present study identified the lncRNA *2810403D21Rik/AK007586/Mirf (myocardial infarction-regulatory factor)*, that inhibited macroautophagy/autophagy by modulating *Mir26a* (microRNA 26a). Inhibition of *Mir26a* led to cardiac injury both *in vitro* and *in vivo*, whereas overexpression of *Mir26a* attenuated ischemic stress-induced cell death by activating autophagy through targeting *Usp15* (ubiquitin specific peptidase 15). More importantly, *2810403D21Rik/Mirf* acted as a competitive endogenous RNA (ceRNA) of *Mir26a*; forced expression of *2810403D21Rik/Mirf* downregulated *Mir26a* to inhibit autophagy. In contrast, loss of *2810403D21Rik/Mirf* resulted in upregulation of *Mir26a* to promote autophagy and alleviate cardiac injury, which in turn improved cardiac function in MI mice. This study identified a lncRNA *2810403D21Rik/Mirf* that functions as an anti-autophagic molecule via ceRNA activity toward *Mir26a*. Our findings suggest that knockdown of *2810403D21Rik/Mirf* might be a novel therapeutic approach for cardiac diseases associated with autophagy.

Abbreviations: 3-MA: 3-methyladenine; AAV-9: adenovirus associated virus-9; ago*Mir26a*: cholesterol-conjugated *Mir26a* mimic; AMI: acute myocardial infarction; *AMO-26a: Mir26a* inhibitor; ATG: autophagy related; BECN1: beclin 1; ceRNA: competitive endogenous RNAs; EF: ejection fraction; f-*2810403D21Rik/Mirf*: fragment encompassing the *Mir26a* binding site; FS: fraction shortening; GFP-mRFP: a plasmid expressing green fluorescent protein-monomeric red fluorescent protein; lncRNA: long non-coding RNA; MAP1LC3/LC3: microtubule-associated protein 1 light chain 3; *Mirf*: myocardial infarction-regulatory factor; miRNAs: microRNAs; *NC*: negative control; NMCMs: neonatal mice cardiomyocytes; shRNA: short hairpin RNA; siRNA: small interfering RNA; SQSTM1/p62: sequestosome 1; TEM: transmission electron microscopy; *Usp15*: ubiquitin specific peptidase 15.

ARTICLE HISTORY
Received 17 July 2018
Revised 30 July 2019
Accepted 9 August 2019

KEYWORDS
Autophagy; lncRNA-*2810403D21Rik/Mirf*; Mir26a; myocardial infarction; Usp15

Introduction

Acute myocardial infarction (AMI), which is induced by acute coronary artery occlusion, is one of the leading causes of death worldwide [1]. Cardiac cell death, along with subsequent excessive inflammation, is the main cause of cardiac injury in AMI, and can eventually lead to heart failure and sudden death [2]. Because cardiomyocytes are terminally differentiated and have little potentiality for division, strategies that prevent the irreversible loss of cardiomyocytes in AMI have great therapeutic value.

Numerous studies have found that autophagy, which is generally thought to be a protective factor against ischemic injury in cardiomyocytes [3,4], is involved in cardiac cell death associated with AMI, though damaged cardiomyocytes exhibit characteristics of macroautophagy/autophagy during heart failure [5]. Our previous study reveals that PPP3/calcineurin (protein phosphatase 3) suppresses cytoprotective autophagy in cardiomyocytes under oxidative stress. Correspondingly, loss of PPP3 restores autophagy and decreases the extent of apoptosis induced by oxidative stress [6]. However, the role of autophagy in the progression of ischemic heart disease is not well understood, and the upstream factors that control autophagy require elucidation.

Non-coding RNAs are a class of RNAs that do not encode proteins [7]. Among non-coding RNAs, microRNAs (miRNAs)

CONTACT : Hongli Shan shanhongli@ems.hrbmu.edu.cn Department of Pharmacology (State-Province Key Laboratories of Biomedicine-Pharmaceutics of China, Key Laboratory of Cardiovascular Research, Ministry of Education), College of Pharmacy, Harbin Medical University, Baojian Road 157, Harbin, Heilongjiang 150081, P. R. China; Zhimin Du dzm1956@126.com Institute of Clinical Pharmacy, The 2nd Affiliated Hospital, Harbin Medical University
*Authors with equal contribution to this study
Supplemental data for this article can be accessed here.

are known to participate widely in numerous biological and pathophysiological coronary processes, such as arrhythmia, myocardial infarction, and cardiac fibrosis [8,9]. Our previous study finds that *Mir1* is a master regulator for arrhythmia, and inhibition of *Mir1* in infarcted rat hearts relieves arrhythmogenesis [9]. *Mir26a* is a highly conserved miRNA and is dysregulated in a number of cardiovascular diseases. For example, overexpression of *Mir26a* offers protection against atrial fibrillation [10], cardiac hypertrophy [11] and endothelial cell apoptosis [12]. However, it remains to be determined whether *Mir26a* is involved in AMI.

Besides miRNAs, it has recently been demonstrated that long non-coding RNAs (lncRNAs) play a crucial role in cardiovascular diseases [13–15]. More interestingly, the cross-regulatory network between miRNAs and lncRNAs has recently been identified, providing insights into the comprehensive functionality of these non-coding transcripts and their potential as therapeutics [16]. However, it remains unclear whether lncRNAs participate in the regulation of cardiomyocyte autophagy.

In the current study we found that *Mir26a* directly targeted *Usp15* (ubiquitin specific peptidase 15), activating autophagy and, thereby, alleviating ischemic stress-induced cardiac injury. Furthermore, we identified lncRNA *2810403D21Rik/AK007586/Mirf* (*myocardial infarction-regulatory factor*), and found that upregulation of this lncRNA induced cardiac injury by inhibiting autophagy through its interactions with *Mir26a*. More importantly, knockdown of *2810403D21Rik/Mirf* mitigated cardiac injury and improved heart function in MI mice. Our results suggest that *2810403D21Rik/Mirf* and *Mir26a* could be novel therapeutic targets for ischemic heart disease.

Results

Cardioprotective effects of Mir26a *in MI: role of autophagy*

To determine whether *Mir26a* participates in progression of cardiac injury, we developed a MI model in mice. Expression of *Mir26a* was decreased in the MI mice after 24 h (Figure 1A), and was also decreased in normal cardiomyocytes treated with H_2O_2 (Figure 1B).

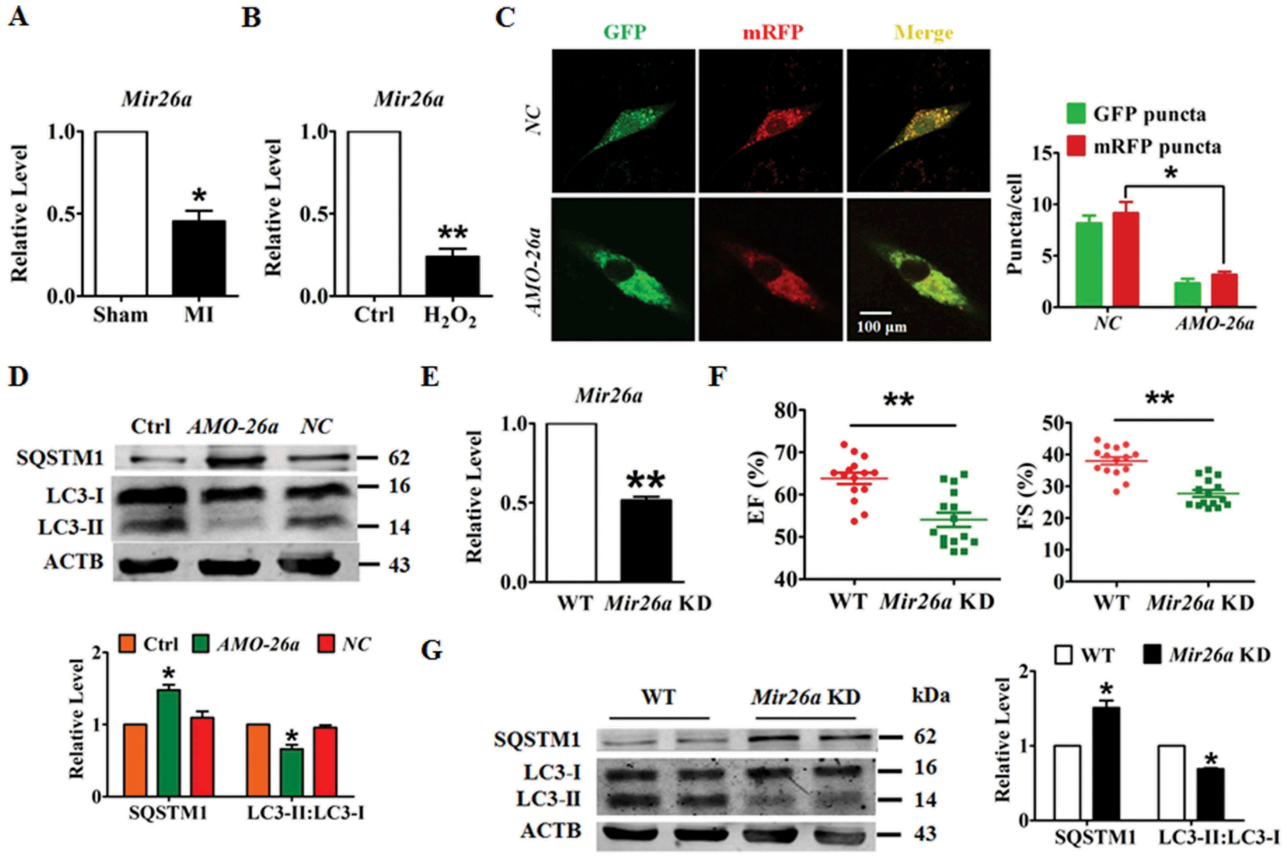

Figure 1. Knockdown of *Mir26a* decreases autophagy to impair heart function. (A) Downregulation of *Mir26a* in the peri-infarct area determined by qRT-PCR. n = 6. *$p < 0.05$ *vs.* Sham. (B) Downregulation of *Mir26a* in cultured neonatal mouse cardiomyocytes (NMCMs) treated with 200 μmol/L H_2O_2 for 12 h. n = 5. **$p < 0.01$ *vs.* Control. (C) Knockdown of *Mir26a* inhibited autophagic flux in NMCMs. NMCMs were transfected with *AMO-26a* for 24 h, followed by transfection of tandem-LC3 construct (GFP-mRFP-LC3) for another 24 h. The images were obtained using a confocal microscope. The yellow and red puncta represent autophagosomes and autolysosomes, respectively. The data were obtained from 3 independent experiments and 10 cells were scored in each experiment. *$p < 0.05$. *NC*, negative control of *AMO-26a*. (D) Knockdown of *Mir26a* increased the level of SQSTM1/p62 protein and reduced the expression of LC3-II, as determined by western blot. n = 5. *$p < 0.05$ *vs.* Control. *NC*, negative control of *AMO-26a*. (E) Downregulation of *Mir26a* in *Mir26a* KD mice. n = 6. **$p < 0.01$ *vs.* WT. (F) Knockdown of *Mir26a* impaired heart function in mice. n = 15. **$p < 0.01$ *vs.* WT. (G) Knockdown of *Mir26a* resulted in the deregulation of autophagy-related proteins in mouse hearts. n = 6. *$p < 0.05$ *vs.* WT.

To examine the role of *Mir26a* in the pathogenesis of ischemic injury in neonatal mice cardiomyocytes (NMCMs), we applied an *Mir26a* inhibitor (*AMO-26a*) to inhibit expression of endogenous *Mir26a*. Meanwhile, a plasmid expressing green fluorescent protein/monomeric red fluorescent protein (GFP-mRFP) in tandem tagged MAP1LC3/LC3 protein were transfected into NMCMs to assess the influence of *Mir26a* inhibition on the final step of autophagic breakdown (autophagosome formation and the autophagosome-lysosome fusion process). Silencing *Mir26a* reduced the number of both autophagosomes (yellow puncta) and autolysosomes (red puncta) in NMCMs (Figure 1C). Consistent with this result, knockdown of *Mir26a* retarded expression of LC3-II and increased expression of SQSTM1/p62 (Figure 1D).

To further investigate the function of *Mir26a* in progression of myocardial infarction, we generated a *Mir26a* sponge transgenic mouse (*Mir26a* KD mice) to knockdown expression of endogenous *Mir26a*. As shown in Figure 1E, the level of *Mir26a* was markedly decreased in the *Mir26a* KD mice. Moreover, silencing of endogenous *Mir26a* reduced the ejection fraction and fraction shortening (EF and FS, respectively; Figure 1F), indicating that *Mir26a* inhibition impaired the left ventricular function. Furthermore, inhibition of *Mir26a* blocked the formation of autophagosomes and caused downregulation of autophagy in the hearts of *Mir26a* KD mice (Figure 1G).

These results indicated that knockdown of *Mir26a* resulted in heart defects in mice. To examine whether overexpression of *Mir26a* has a beneficial effect on the pathogenesis of ischemic injury in cardiomyocytes, we transfected *Mir26a* mimics into NMCMs. Overexpression of *Mir26a* alleviated H_2O_2-induced inhibition of cell viability in NMCMs, inhibition which was abolished by the autophagy antagonist 3-methyladenine (3-MA). No significant changes were elicited in the negative control (Figure 2A). Meanwhile, enhanced expression of *Mir26a* promoted formation of autophagosomes and autophagosome-lysosome fusion. Notably, this effect was attenuated if autophagy had been inhibited by 3-MA (Figure 2B and Figure S1A). To further examine whether autophagy is necessary for the protective effect of *Mir26a*, autophagy flux in NMCMs was blocked by application of siRNA against *Atg5* or treated with either chloroquine or pepstatin A-E64d. Blocking autophagy diminished the pro-survival and pro-autophagic effects of *Mir26a* in H_2O_2-treated cardiomyocytes (Figure S1B,C).

To assess whether *Mir26a* activates autophagy to mitigate ischemic myocardial injury we injected a cholesterol-conjugated *Mir26a* mimic (ago*Mir26a*) through the tail-vein into mice for overexpression, and then created MI conditions in the mice. As expected, overexpression of *Mir26a* improved heart function and reduced infarct size in the model MI mouse (Figure 2C,D). Promotion of autophagy by *Mir26a* in MI mice was observed directly by transmission electron microscopy (Figure 2E). In accordance with these results, western blot showed that forced expression of *Mir26a* promoted expression of proteins related to autophagy in MI mice (Figure 2F).

Signaling mechanisms for the cardioprotective effects Mir26a: *repression of* Usp15

To delineate the downstream signaling mechanisms responsible for the beneficial effects of *Mir26a*, the TargetScan miRNA database (http://www.targetscan.org/vert_71/) was used for identification of autophagy-related genes that could be targeted by *Mir26a*. Computational -analyzes identified that the gene encoding *Usp15*, which is broadly conserved among human, mouse and rat species, contains the seed sequence for *Mir26a* (Figure 3A). *Usp15* has previously been reported to antagonize mitophagy in fibroblasts of patients [17], and, intriguingly, was upregulated in the border zone of MI hearts and in the cardiomyocytes exposed to H_2O_2 (Figure 3B,C).

Subsequent experiments validated the direct regulatory effect of *Mir26a* on *Usp15*. Luciferase expression vectors carrying the wild-type (WT) *Mir26a* binding sites or one of the mutated versions of the *Mir26a* binding sites (Figure 3A) were constructed. Overexpression of *Mir26a* by co-transfection inhibited luciferase activity by the luciferase vectors carrying the WT *Usp15* binding sites or the mutation in binding site 1 (mut-1), but not by the luciferase vectors carrying mutations in site 2 (mut-2) or both sites 1 and 2 (mut-3) (Figure 3D). This suggests that the binding site 2 of *Usp15* might play the major role in *Mir26a* regulation of *Usp15*. Moreover, the level of USP15 proteins was reduced by *Mir26a* but increased by *AMO-26a*, although neither affected transcription of *Usp15* (Figure 3E,F). Consistent with the *in vitro* study, expression of USP15 was also increased in *Mir26a* KD mice (Figure 3G). More importantly, overexpression of *Mir26a* in NMCMs inhibited expression of SQSTM1/p62 and promoted expression of LC3-II, ATG7, BECN1/Beclin1, and ATG5 (Figure 3H).

To determine whether *Mir26a* promotes cardiac autophagy through *Usp15*, we constructed siRNA against *Usp15* to inhibit endogenous *Usp15* expression. Inhibition of *Mir26a* caused a decrease in cell viability that could be rescued by *Usp15* knockdown (Figure S2A). Silencing *Usp15* also attenuated the inhibitory effect of *Mir26a* inhibition on autophagosomes and autolysosomes formation (Figure S2B). Furthermore, western blot analysis showed that knockdown of *Mir26a* resulted in higher expression of USP15, SQSTM1 and downregulation of LC3-II:LC3-I, ATG7, BECN1, and ATG5. Changes in protein expression by *Mir26a* knockdown were all relieved by *Usp15*/USP15 inhibition (Figure S2C). These results show that *Mir26a* regulated autophagy in cardiomyocytes by targeting *Usp15*.

LncRNA 2810403D21Rik/Mirf *is able to bind to and regulate activity of* Mir26a

Evidence is mounting that lncRNAs act as ceRNA (competitive endogenous RNA) that competitively bind to and restrain the activity of miRNAs [18]. To determine whether lncRNAs inhibit expression of *Mir26a* in the murine MI model, we used the miRanda database (http://www.microrna.org/microrna/getMirnaForm.do) to identify lncRNA in mice with *Mir26a* biding sites. The candidate lncRNAs were filtered based on their expression profiles in the MI mouse (GSE46395) and their expression profiles were tested by qRT-PCR. The lncRNA *AK007586* (Ensembl ID: ENSMUSG00000086629), which was significantly upregulated in the MI mice (Figure 4A), was selected for further analysis and designated *2810403D21Rik/*

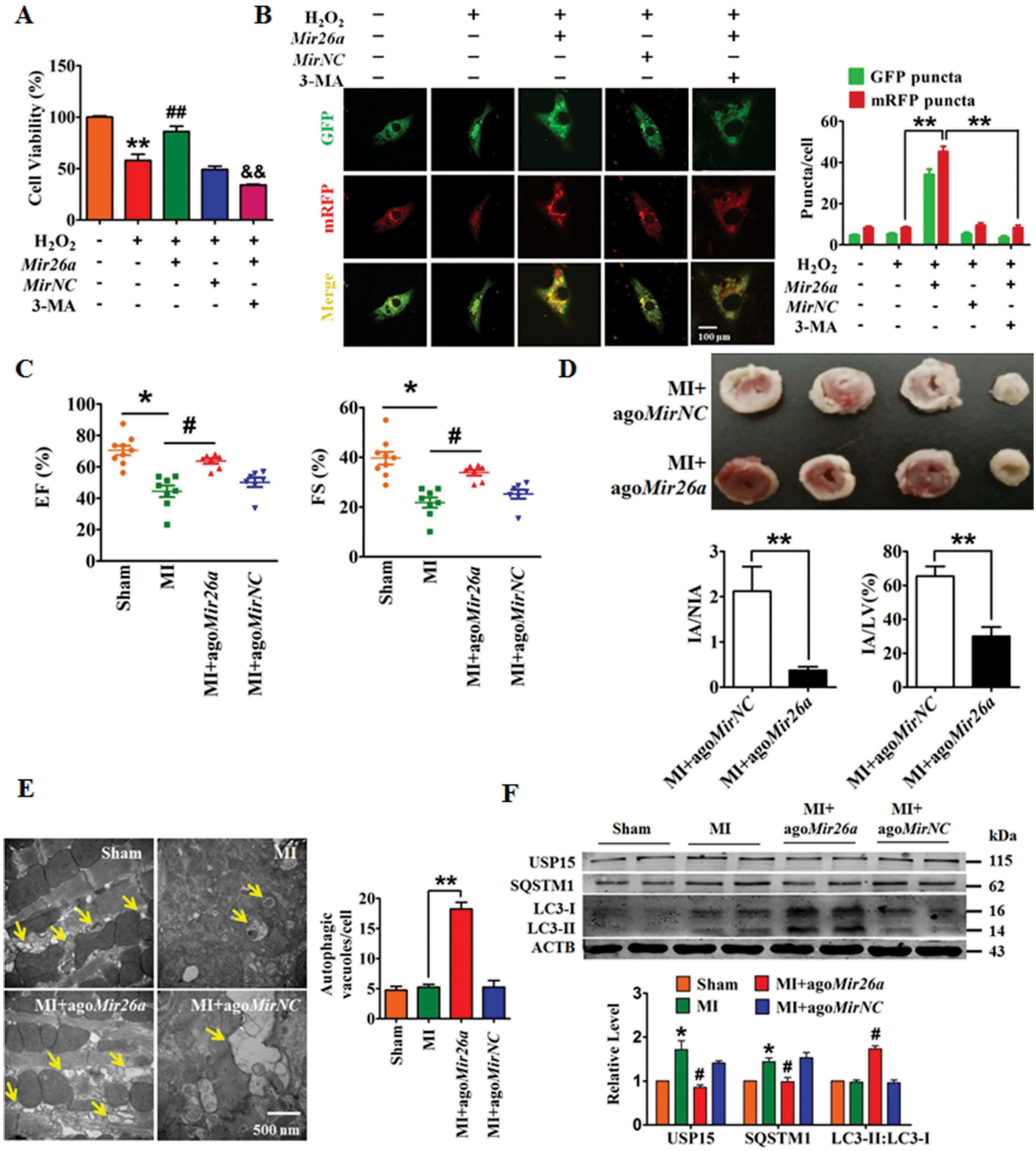

Figure 2. Forced expression of *Mir26a* protects cardiomyocytes from injury by activating autophagy. (A) Overexpression of *Mir26a* alleviated H_2O_2-induced inhibition of cell viability in NMCMs. This effect was reversed by application of 3-MA, an autophagic antagonist. n = 8. $^{**}p < 0.01$ *vs*. Control; $^{\#\#}p < 0.01$ *vs*. H_2O_2; $^{\&\&}p < 0.01$ *vs*. H_2O_2+ *Mir26a*. *MirNC*, negative control of *Mir26a*. (B) Forced expression of *Mir26a* restored the inhibition of autophagy induced by H_2O_2. Data were obtained from 3 independent experiments and 10 cells were scored in each experiment. $^{**}p < 0.01$. *MirNC*, negative control of *Mir26a*. (C) Overexpression of *Mir26a* improved heart function (n = 9. $^{*}p < 0.05$ *vs*. Sham; $^{\#}p < 0.05$ *vs*. MI) and reduced the infarct size (both IA/NIA and IA/LV) in MI mice (D) (n = 9. $^{**}p < 0.01$ *vs*. MI+ago *MirNC*). (E) Overexpression of *Mir26a* enhanced autophagic activity in MI mice. n = 5. $^{**}p < 0.01$ *vs*. MI. AgomiR-NC, negative control of ago*Mir26a*. (F) Overexpression of *Mir26a* normalized the dysregulated expression of autophagy-related proteins in MI mice. n = 6. $^{*}p < 0.05$ *vs*. Sham; $^{\#}p < 0.05$ *vs*. MI. Ago *MirNC*, negative control of ago*Mir26a*.

Mirf. Expression of *2810403D21Rik/Mirf* was significantly increased in NMCMs after treatment with H_2O_2 (Figure 4B). In addition, we found that *2810403D21Rik/Mirf* was mainly located in the cytoplasm of NMCMs (Figure 4C). Overexpression of *2810403D21Rik/Mirf* inhibited expression of *Mir26a* in NMCMs (Figure 4D), whereas silencing of *2810403D21Rik/Mirf* by specific short hairpin RNA (shRNA) resulted in *Mir26a* upregulation (Figure 4E).

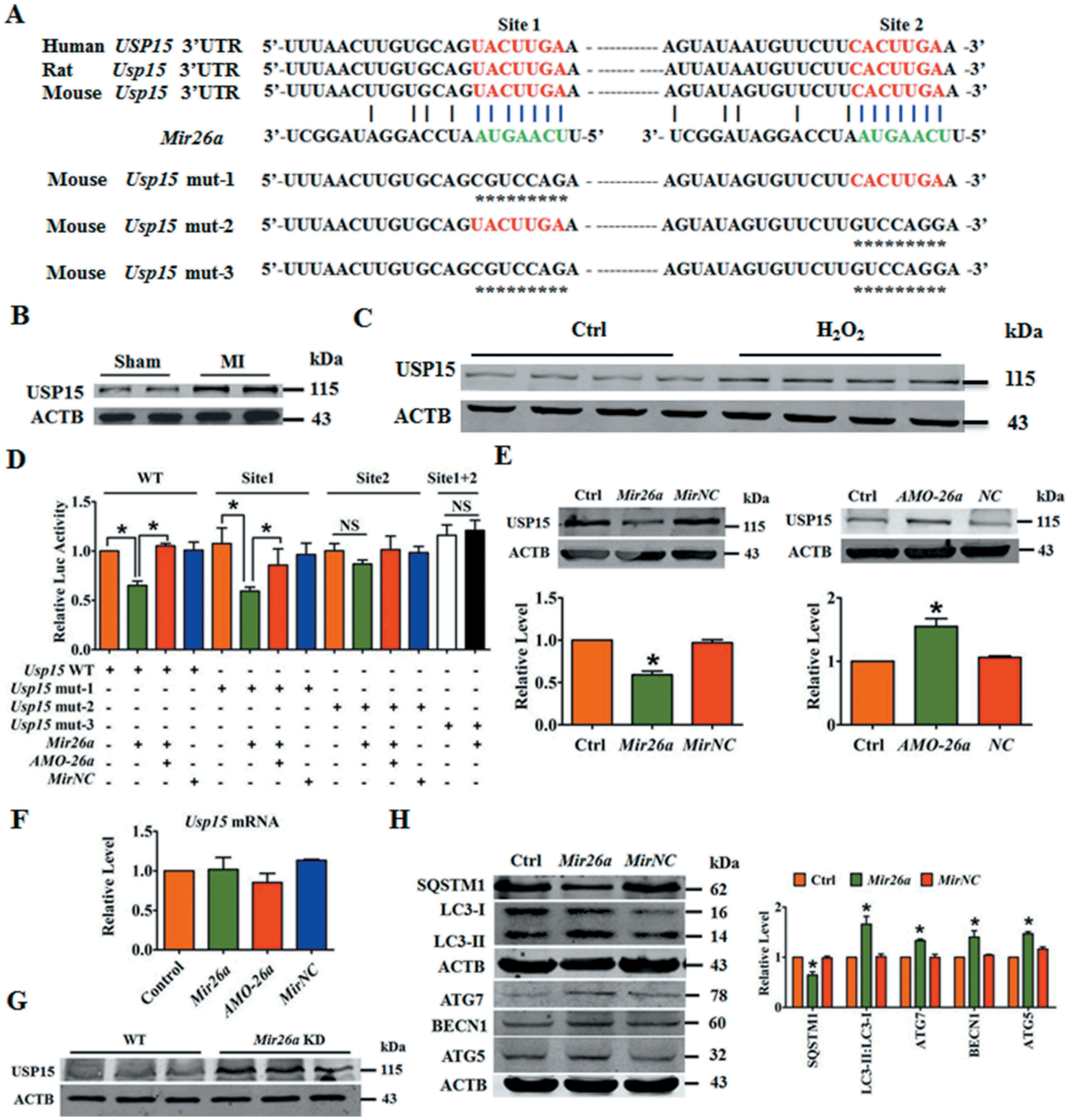

Figure 3. *Usp15* is a direct target of *Mir26a*. (A) Sequence alignment showing complementarity between mouse, rat, and human *Mir26a* and *Usp15* genes. The matched base pairs in the seed region are outlined by red and green. (B) Increased expression of USP15 in infarct border area in MI mice. n = 6. $^{**}p < 0.01$ *vs*. Sham. (C) Increased expression of USP15 in NMCMs after treatment with 200 μmol/L H_2O_2 for 12 h. n = 6. (D) Luciferase reporter activity of chimeric vectors carrying a luciferase gene and a fragment of the *Usp15* 3′-UTR containing the wild-type or mutant binding sites for *Mir26a* were detected in HEK293 cell line. n = 6. $^{*}p < 0.05$. *MirNC*, negative control of *Mir26a*. (E) Overexpression of *Mir26a* depressed protein levels of USP15 (n = 6. $^{*}p < 0.05$ *vs*. Control. *MirNC*, negative control of *Mir26a; NC*, negative control of *AMO-26a*), (F) but did not affect its mRNA levels (n = 6). (G) Upregulation of USP15 in *Mir26a* KD mice, the three lanes of WT and KD correspond to three different mice. n = 6. $^{**}p < 0.01$ *vs*. Sham. (H) Forced expression of *Mir26a* inhibited expression of SQSTM1 and promoted the transition of LC3-I into LC3-II. n = 6. $^{*}p < 0.05$ *vs*. Control. *MirNC*, negative control of *Mir26a*.

To further characterize the relationship between *2810403D21Rik/Mirf* and *Mir26a*, a *Mir26a* sensor luciferase vector containing a fragment of the *2810403D21Rik/Mirf* sequence that included the *Mir26a* binding site incorporated into the 3′-UTR of the luciferase gene was constructed (Figure 4F). Overexpression of *2810403D21Rik/Mirf* increased luciferase activity and silencing of *2810403D21Rik/Mirf* had the opposite effect (Figure 4G), indicating that *2810403D21Rik/Mirf* could bind to *Mir26a* and reduce the availability of functional *Mir26a*. Furthermore, *Mir26a* significantly inhibited the luciferase activity of the sensor vector, inhibition which was alleviated by co-expression of WT *2810403D21Rik/Mirf*. The mutated *2810403D21Rik/Mirf* (mut-*2810403D21Rik/Mirf*), which lacked the *Mir26a* binding site, failed to alleviate inhibition of luciferase activity by *Mir26a* (Figure 4H). More importantly, overexpression of *Mir26a* suppressed luciferase activity of the WT

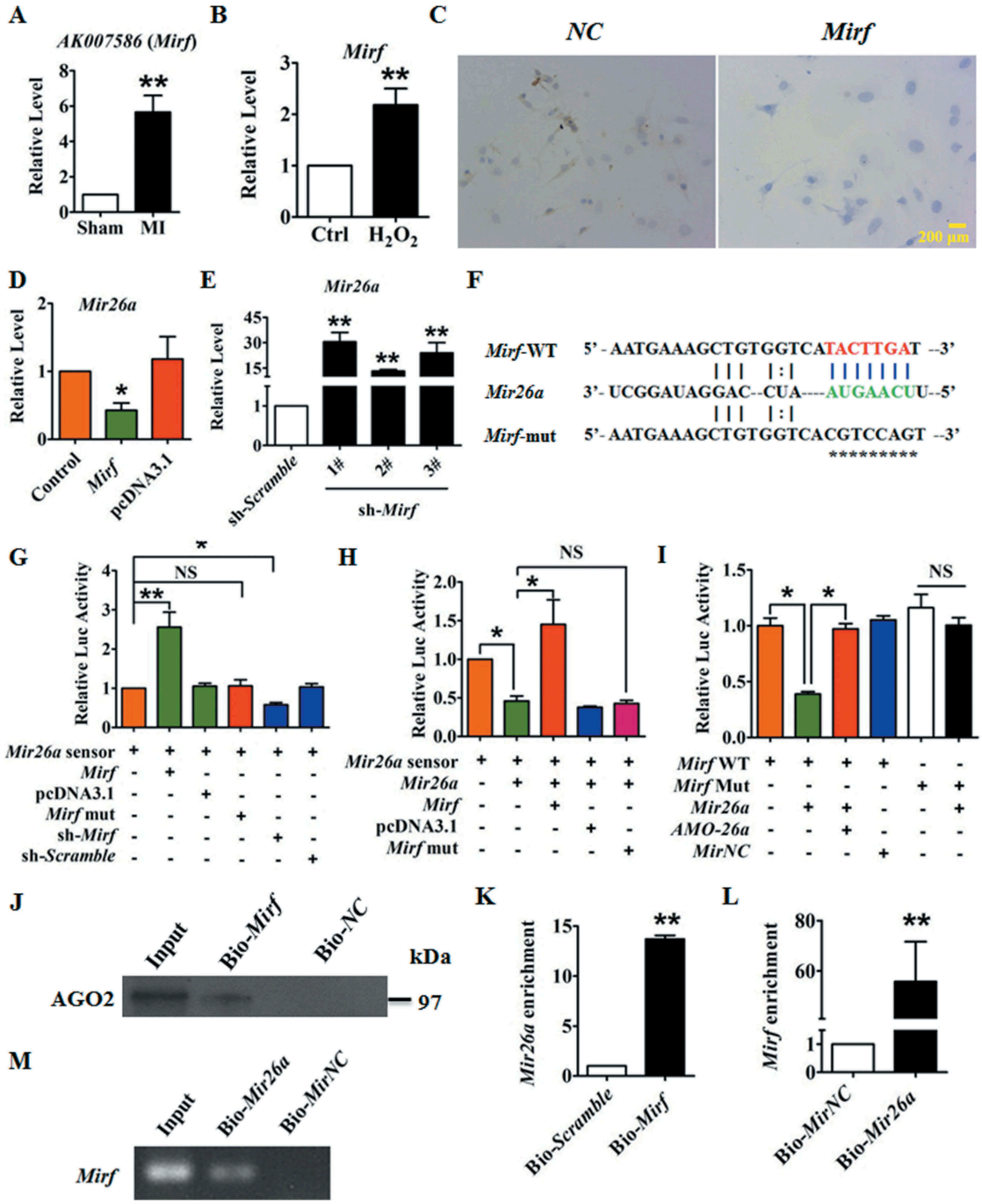

Figure 4. LncRNA *2810403D21Rik/Mirf* regulates the expression and activity of *Mir26a*. (A) Upregulation of *2810403D21Rik/Mirf* in MI mice. n = 6. $^{**}p < 0.01$ *vs*. Sham. (B) Upregulation of *2810403D21Rik/Mirf* in NMCMs after treatment with 200 μmol/L H_2O_2 for 12 h. n = 6. $^{**}p < 0.01$ *vs*. Control. (C) *In situ* hybridization showed the location of *2810403D21Rik/Mirf* in NMCMs. (D) Overexpression of *2810403D21Rik/Mirf* downregulated *Mir26a*. n = 6. $^{*}p < 0.05$ *vs*. Control. pcDNA3.1, negative control. (E) Silencing of *2810403D21Rik/Mirf* by the specific shRNA upregulated *Mir26a*. The black bar indicates three different shRNA sequences against *2810403D21Rik/Mirf*. n = 6. $^{**}p < 0.01$ *vs*. sh-*Scramble*. sh-*Scramble*, negative control of sh-*2810403D21Rik/Mirf*. (F) *2810403D21Rik/Mirf* contained a sequence domain complementary to the seed motif of *Mir26a*. (G and H) *2810403D21Rik/Mirf* binds to *Mir26a* and regulates its activity in NMCMs. n = 6. $^{*}p < 0.05$, $^{**}p < 0.01$. (I) Luciferase reporter activities of chimeric vectors carrying luciferase gene and a fragment of *2810403D21Rik/Mirf* RNA containing WT binding site or mutant binding site for *Mir26a* were detected in HEK293 cell line. n = 6. $^{*}p < 0.05$. pcDNA3.1, negative control of *2810403D21Rik/Mirf*. sh-*Scramble*, negative control of sh-*2810403D21Rik/Mirf*. *MirNC*, negative control of *Mir26a*. (J) RNA affinity isolation in NMCMs using biotin-labeled *2810403D21Rik/Mirf* probes. Western blot was used to detected enrichments of AGO2. n = 3. (K) *Mir26a* was pulled down by *2810403D21Rik/Mirf* probe, and the expression of *Mir26a* was analyzed by qRT-PCR. Cardiomyocytes were transfected with biotinylated *Mir26a* and then harvested for biotin-based affinity-isolation assay. n = 6. $^{**}p < 0.01$. *Scramble*, negative control of *2810403D21Rik/Mirf*. (L) *2810403D21Rik/Mirf* was pulled down by *Mir26a* as analyzed by real-time RT-PCR. n = 6. $^{**}p < 0.01$. *MirNC*, negative control of *Mir26a*. (M) The product of real-time RT-PCR was identified by agarose gel electrophoresis. *MirNC*, negative control of *Mir26a*.

2810403D21Rik/Mirf luciferase vector, but not of the mut-*2810403D21Rik/Mirf* luciferase vector (Figure 4I).

Next, we constructed a biotin-labeled *2810403D21Rik/Mirf*-specific probe and performed an RNA affinity-isolation assay to test whether *2810403D21Rik/Mirf* could pull down *Mir26a*. It has been found that miRNA, miRNA target RNA, and AGO2 form the RNA-induced silencing complex (RISC) to mediate miRNA-induced gene silencing [19]. The RNA

affinity-isolation assay showed that *2810403D21Rik/Mirf* interacted with AGO2 (Figure 4J). Furthermore, qRT-PCR revealed binding of *2810403D21Rik/Mirf* to *Mir26a* (Figure 4K), indicating that *Mir26a* and *2810403D21Rik/Mirf* interacted with AGO2. We also applied a biotin-avidin affinity-isolation system to test whether *Mir26a* could pull down *2810403D21Rik/Mirf*. Cardiomyocytes were transfected with biotinylated *Mir26a* and then harvested for a biotin-based affinity-isolation assay in which *2810403D21Rik/Mirf* was pulled down by *Mir26a*, as determined by qRT-PCR (Figure 4L) and agarose gel electrophoresis (Figure 4M), indicating that the recognition of *Mir26a* to *2810403D21Rik/Mirf* is sequence specific. Taken together these results suggest that *2810403D21Rik/Mirf* interacts directly with *Mir26a* and AGO2 to form RISC and regulate the expression and activity of *Mir26a*.

LncRNA 2810403D21Rik/Mirf *as a regulator of autophagy through the* Mir26a-Usp15 *axis*

NMCMs were transfected with *2810403D21Rik/Mirf* to verify that *2810403D21Rik/Mirf* contributed to the process of myocardial injury and determine whether this effect was mediated by *Mir26a*. Overexpression of *2810403D21Rik/Mirf* significantly reduced the viability of NMCMs and aggravated H_2O_2-provoked inhibition of cell viability, while this effect was partly alleviated by *Mir26a* or si-*Usp15* (Figure 5A,B). As expected, forced expression of mut-*2810403D21Rik/Mirf* did not affect cell viability (Figure 5A). Furthermore, forced expression of *2810403D21Rik/Mirf* reduced the number of autophagosomes and autolysosomes in NMCMs (Figure 5C), whereas mut-*2810403D21Rik/Mirf* failed to do so. Overexpression of *2810403D21Rik/Mirf* increased expression of SQSTM1 and USP15 and blocked expression of LC3-II, ATG7, BECN1 and ATG5 (Figure 5D and Figure S3), indicating that *2810403D21Rik/Mirf* suppresses autophagy in cardiomyocytes. Moreover, forced expression of *Mir26a* or silencing *Usp15* mitigated the inhibition of autophagy by *2810403D21Rik/Mirf* (Figure 5C,D and Figure S3). These results suggest that *2810403D21Rik/Mirf* limits the functionality of the *Mir26a/Usp15* axis, thereby depressing autophagy and causing myocardial injury via mitigation of intrinsic cardioprotective activity.

We then examined the potential for silencing of *2810403D21Rik/Mirf* to exert a protective effect against cardiac injury in NMCMs exposed to H_2O_2. H_2O_2 attenuated cell viability, an effect that was alleviated by silencing *2810403D21Rik/Mirf*, whereas knockdown of *Mir26a* or inhibition of autophagy using 3-MA abolished the beneficial action of *2810403D21Rik/Mirf* knockdown (Figure 6A). Consistently, blocking autophagy using si-*Atg5*, chloroquine or pepstatin A/E64d consistently restored the regulatory action of *2810403D21Rik/Mirf* knockdown on cell viability in H_2O_2-treated NMCMs (Figure 6B). Moreover, a western blot showed that knockdown of *2810403D21Rik/Mirf* restored the H_2O_2-induced upregulation of autophagy-related proteins SQSTM1 and USP15, and promoted expression of LC3-II, ATG7, BECN1 and ATG5. These regulatory changes were abated by addition of *AMO-26a* or 3-MA (Figure 6C). Blocking autophagy using si-*Atg5*, chloroquine or pepstatin A/E64d consistently restored the regulatory action of *2810403D21Rik/Mirf* on autophagy-related proteins in H_2O_2-treated NMCMs (Figure S4). In agreement with these results, silencing of *2810403D21Rik/Mirf* mitigated the H_2O_2-induced inhibition of autophagy in NMCMs, inhibition which was effectively restored by addition of the *Mir26a* inhibitor or 3-MA (Figure 6D). These data show that silencing of *2810403D21Rik/Mirf* protected against H_2O_2-induced cardiomyocytes injury by activating *Mir26a* and autophagy.

To identify the sequence domain of *2810403D21Rik/Mirf* responsible for the observed ceRNA action toward *Mir26a*, we synthesized a 25 nt *2810403D21Rik/Mirf* fragment (f-*2810403D21Rik/Mirf*) encompassing the *Mir26a* binding site (see the *2810403D21Rik/Mirf*-WT in Figure 4F). Similar to the full-length *2810403D21Rik/Mirf*, f-*2810403D21Rik/Mirf* retained the ability to inhibit the viability of cardiac cells and the effect was abrogated by *Mir26a* (Figure 7A). Meanwhile, overexpression of f-*2810403D21Rik/Mirf* significantly reduced punctate accumulations of GFP-mRFP-LC3, whereas co-transfection of *Mir26a* alleviated the effects of f-*2810403D21Rik/Mirf* and promoted accumulation of autophagosomes and autolysosomes in NMCMs (Figure 7B). Moreover, forced expression of f-*2810403D21Rik/Mirf* increased expression of SQSTM1 and USP15, and inhibited expression of LC3-II, ATG7, BECN1 and ATG5; effects which were almost entirely reversed by *Mir26a* (Figure 7C). These results suggest that f-*2810403D21Rik/Mirf* could mimic the actions of *2810403D21Rik/Mirf* on autophagy and cell injury, indicating that the *Mir26a* binding site is the functional domain of *2810403D21Rik/Mirf*.

Silencing of 2810403D21Rik/Mirf *mitigates myocardial injury and protects heart function in mice subjected to myocardial infarction*

We injected adenovirus associated virus (AAV)-9 carrying the *2810403D21Rik/Mirf*-specific shRNA into mice and evaluated the effects of *2810403D21Rik/Mirf* inhibition on cardiac damage in a mouse model of MI. Knockdown of *2810403D21Rik/Mirf* through tail-vein injection of AAV9-sh-*2810403D21Rik/Mirf* induced upregulation of *Mir26a* in WT mice (Figure 8A), consistent with data from *in vitro* experiments. Moreover, loss of *2810403D21Rik/Mirf* improved the heart function of and diminished the infarct size in mice after MI (Figure 8B,C). Meanwhile, knockdown of *2810403D21Rik/Mirf* increased the number autophagic vesicles (arrows) and promoted cardiac autophagy in MI hearts (Figure 8D). In addition, a western blot showed that inhibition of *2810403D21Rik/Mirf* in MI mice restored the upregulation of SQSTM1 and USP15, rescued the downregulating of ATG7, BECN1 and ATG5, and promoted the transition of LC3-I into LC3-II (Figure 8E). These results suggest that silencing of *2810403D21Rik/Mirf* might regulate autophagy and afford protective effects against ischemic damage of cardiac function.

Discussion

The present study established that the lncRNA *2810403D21Rik/Mirf* was a damaging factor in MI, whereas *Mir26a* was

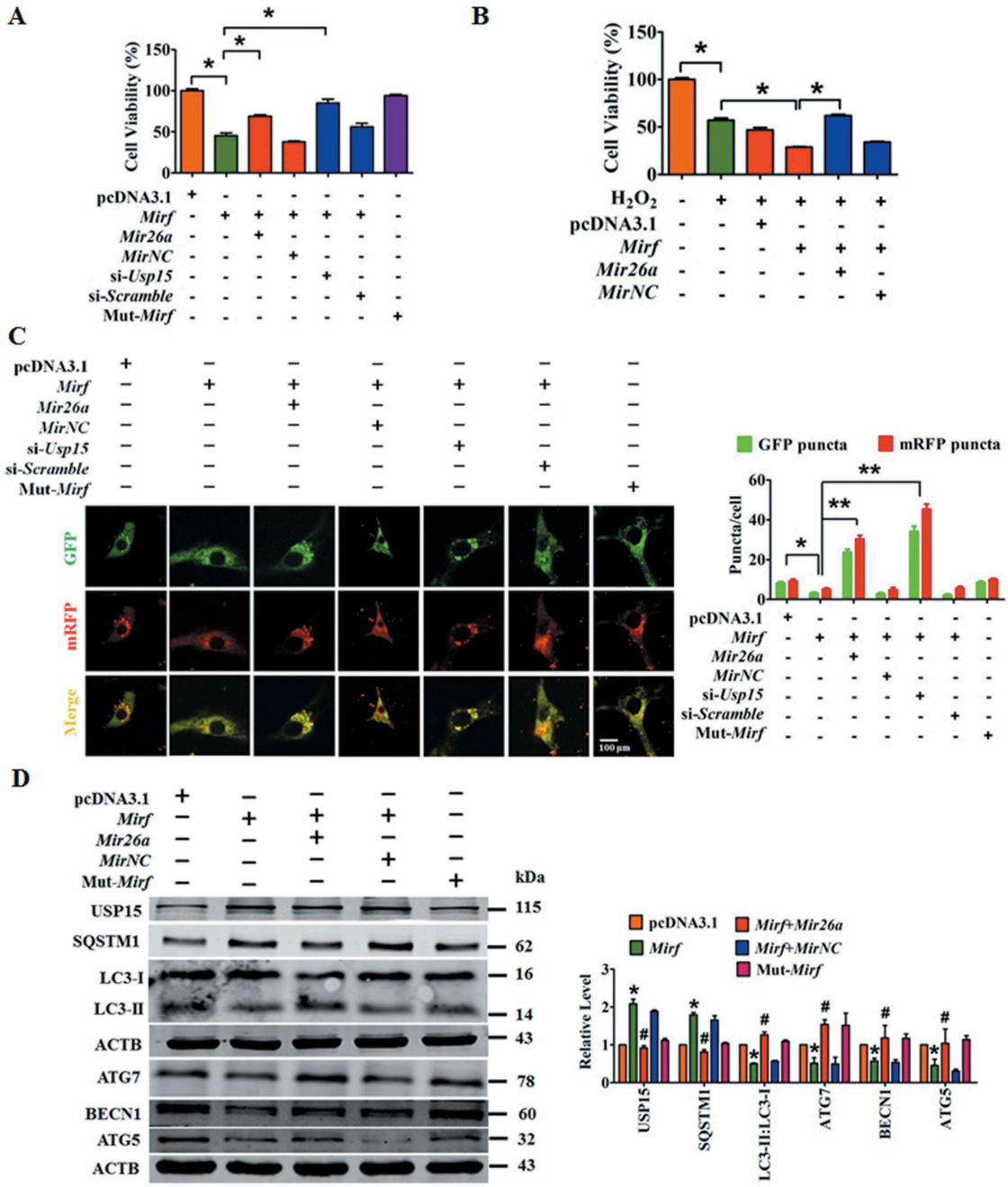

Figure 5. *2810403D21Rik/Mirf* modulated autophagy by regulating *Mir26a* and *Usp15*, promoting cardiac injury in NMCMs. (A) Overexpression of *2810403D21Rik/Mirf* decreased viability of NMCMs; this effect was attenuated by *Mir26a* or si-*Usp15*. n = 5. *$p < 0.05$. pcDNA3.1, negative control of *2810403D21Rik/Mirf*. *MirNC*, negative control of *Mir26a*. si-*Scramble*, negative control of si-*Usp15*. (B) *2810403D21Rik/Mirf* aggravated H_2O_2-induced cardiac injury in NMCMs. n = 6. *$p < 0.05$. pcDNA3.1, negative control of *2810403D21Rik/Mirf*. *MirNC*, negative control of *Mir26a*. (C) Overexpression of *2810403D21Rik/Mirf* blocked the autophagic activity of NMCMs. n = 10. *$p < 0.05$, **$p < 0.01$. pcDNA3.1, negative control of *2810403D21Rik/Mirf*. *MirNC*, negative control of *Mir26a*. si-Scramble, negative control of si-*Usp15*. (D) Overexpression of *2810403D21Rik/Mirf* produced anti-autophagic action through regulation of various relevant proteins, which was abolished by *Mir26a*. n = 5. *$p < 0.05$ *vs.* pcDNA3.1; #$p < 0.05$ *vs. 2810403D21Rik/Mirf*. pcDNA3.1, negative control of *2810403D21Rik/Mirf*. *MirNC*, negative control of *Mir26a*.

a protective miRNA in MI. That is, *2810403D21Rik/Mirf* exaggerated and *Mir26a* attenuated ischemic cardiac injury through modulation of autophagy. Moreover, reciprocal alterations in the expression of these two non-coding RNAs (upregulation of *2810403D21Rik/Mirf* and downregulation of *Mir26a*) in the ischemic zones of MI hearts were observed. The opposite functionalities and reciprocal expression of *2810403D21Rik/Mirf* and *Mir26a* could be well explained by ceRNA regulation, in which the former acts as a sponge to limit the availability of the latter. In addition, we found that *Mir26a* plays a protective role in ischemic injury in cardiomyocytes at least in part by directly targeting regulation of USP15. Notably, both silencing *2810403D21Rik/Mirf* and overexpressing *Mir26a* reduced the infarcted area and improved cardiac function. These findings lead to the conclusion that *2810403D21Rik/Mirf* is a novel anti-autophagic lncRNA that absorbs the pro-autophagic miRNA *Mir26a*, which can exaggerate ischemic cardiac injury by relieving repression of anti-autophagic protein USP15 (Figure 8F). Both *2810403D21Rik/Mirf* and *Mir26a*

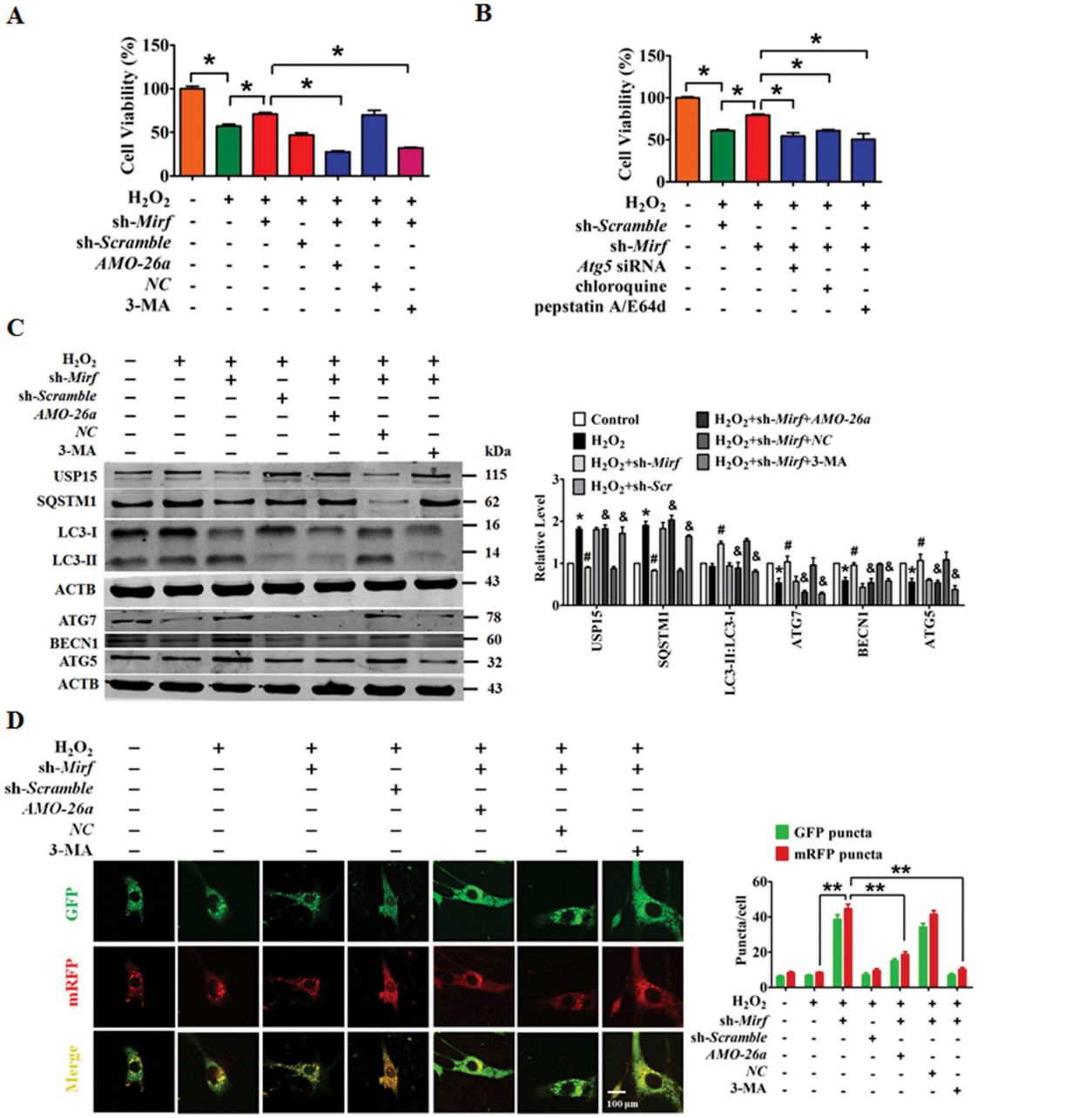

Figure 6. Inhibition of *2810403D21Rik/Mirf* antagonizes H_2O_2-induced injury in NMCMs through modulation of autophagy by increasing *Mir26a*. (A) Silencing of *2810403D21Rik/Mirf* alleviated H_2O_2-induced cardiac injury, which was reversed by knockdown of *Mir26a* by *AMO-26a* or inhibition of autophagy by 3-MA in NMCMs. n = 6. *$p < 0.05$. sh-*Scramble*, negative control of sh-*2810403D21Rik/Mirf*. *NC*, negative control of *AMO-26a*. (B) Inhibition of autophagy by si-*Atg5*, chloroquine or pepstatin A/E64d mitigated the pro-survival effects of *2810403D21Rik/Mirf* silencing in H_2O_2-treated NMCMs. n = 6. *$p < 0.05$. (C) Knockdown of *2810403D21Rik/Mirf* restored abnormal expression of autophagy-related proteins induced by H_2O_2. n = 5. *$p < 0.05$ *vs*. or Control; $^{\#}p < 0.05$ *vs*. H_2O_2; $^{\&}p < 0.05$ *vs*. H_2O_2+ sh-*2810403D21Rik/Mirf*. sh-*Scramble*, negative control of sh-*2810403D21Rik/Mirf*. *NC*, negative control of *AMO-26a*.(D) Silencing of *2810403D21Rik/Mirf* promoted autophagy through increasing expression of *Mir26a*. The data were obtained from 3 independent experiments and 10 cells were scored in each experiment. **$p < 0.01$. sh-*Scramble*, negative control of sh-*2810403D21Rik/Mirf*. *NC*, negative control of *AMO-26a*.

might be considered as potential non-coding RNA targets for the treatment of cardiac diseases associated with autophagy.

Cardiovascular disease, especially AMI, is one of the major causes of death worldwide and its morbidity is increasing year by year [20]. Though our understanding of the pathogenesis of AMI has improved, there are still no effective methods for prevention and treatment. Thus, explorations of new therapeutic approaches at the molecular level are necessary. For the past decade, miRNAs have received worldwide attention for their active participation in various physiological and pathological cardiac processes [21]. Specifically, *Mir26a* has been shown to act against atrial fibrillation and cardiac fibrosis [10,22], hence we investigated whether *Mir26a* has a similarly protective role in AMI. In this work we found that expression of *Mir26a* was decreased in mouse models of ischemic injury and in cardiomyocytes injured by H_2O_2. Overexpressing *Mir26a* improved the cardiac function and cardiomyocytes viability both *in vivo* and *in vitro*, respectively.

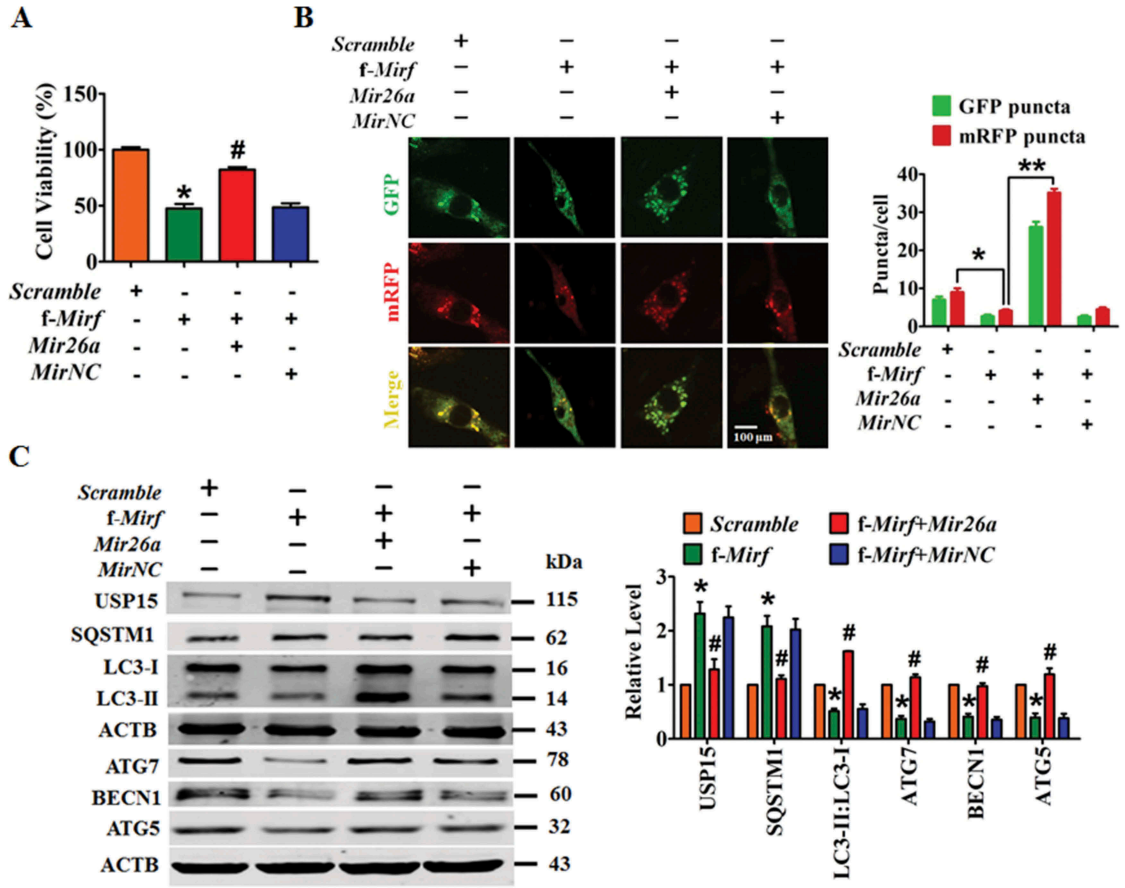

Figure 7. Overexpression of f-*2810403D21Rik/Mirf* provokes myocardial injury in cultured cardiomyocytes by inhibiting endogenous *Mir26a*. (A) Introduction of f-*2810403D21Rik/Mirf*, a 25 nt fragment of the *2810403D21Rik/Mirf* sequence which contained the binding sites of *Mir26a*, inhibits the viability of NMCMs. n = 6. **p* < 0.05 *vs*. Scramble; #*p* < 0.05 *vs*. f-*2810403D21Rik/Mirf*. *Scramble*, negative control of f-*2810403D21Rik/Mirf*. *MirNC*, negative control of *Mir26a*. (B) A confocal assay showed the anti-autophagic effects of f-*2810403D21Rik/Mirf* in NMCMs and could be abrogated by introduction of *Mir26a*. The data were obtained from 3 independent experiments and 10 cells were scored in each experiment. **p* < 0.05, ***p* < 0.01. *Scramble*, negative control of f-*2810403D21Rik/Mirf*. *MirNC*, negative control of *Mir26a*. (C) Forced expression of f-*2810403D21Rik/Mirf* disrupts the expression of autophagy-related proteins by regulation of *Mir26a*. n = 6. **p* < 0.05 *vs*. Scramble; #*p* < 0.05 *vs*. f-*2810403D21Rik/Mirf*. *Scramble*, negative control of f-*2810403D21Rik/Mirf*. *MirNC*, negative control of *Mir26a*.

Thus, our study expands the range of known protective effects of *Mir26a* against ischemic heart injuries.

Autophagy is an important process in aging, inflammation, tumor metabolism and cardiovascular diseases [23]. In cardiomyocytes autophagy maintains the renewal of mitochondria, helping to meet the energy demands of the heart [24]. Because of their non-dividing nature, cardiomyocytes are highly dependent on autophagy for the renewal of non-functional mitochondria, proteins and other organelles. However, the roles of autophagy in MI are still a matter of debate. Autophagy can be either protective or maladaptive in MI, depending on the context of stress. Some studies have found that autophagy is detrimental and that abnormal autophagy is associated with myriad diseases, including cardiovascular disease [25,26]. However, an increasing amount of evidence has demonstrated that activation of autophagy in cardiomyocytes is an adaptive response to stimuli and that inhibiting autophagy accelerates heart failure [27]. Zhang *et al.* found that BAG3 promotes cell proliferation and inhibits apoptosis by activating autophagy in cardiomyocytes injury induced by hypoxia [28]. Also, cardiac-specific over-expression of *Mir221*, which inhibits autophagy by modulating the CDKN1B-CDK2-MTOR axis, in mice promotes heart failure [29]. Our present work focused on identifying the role of *Mir26a* in regulating autophagy, finding that *Mir26a* enhanced cell viability and suppressed cardiac injury by autophagy at least in part by targeting regulation of *Usp15*.

It has been well demonstrated that lncRNAs participate in multiple human diseases by acting as sponges to reduce the expression levels of miRNAs and correspondingly increase the levels of target genes [30]. The lncRNA *Chast* (cardiac hypertrophy-associated transcript) is reported to impede cardiomyocyte autophagy and drive cardiac hypertrophy [31] and another, *Chaer1* (cardiac hypertrophy associated epigenetic regulator 1), negatively regulates AEBP2/PRC2 function and induces cardiac hypertrophy by defining an epigenetic checkpoint [32]. *LOC100129973* has been found to suppress apoptosis by sponging *Mir4707-5p* and *Mir4767* in vascular endothelial cells [33]. These reports demonstrate that lncRNAs can interact with miRNAs to exert biological functions. In the present study, we found that lncRNA *2810403D21Rik/Mirf* is a distinct ceRNA for *Mir26a*. Expression of *2810403D21Rik/Mirf* was significantly increased in MI hearts and H_2O_2 treated cardiomyocytes, suggesting meaningful participation of *2810403D21Rik/Mirf* in MI. Theoretically, ceRNAs should

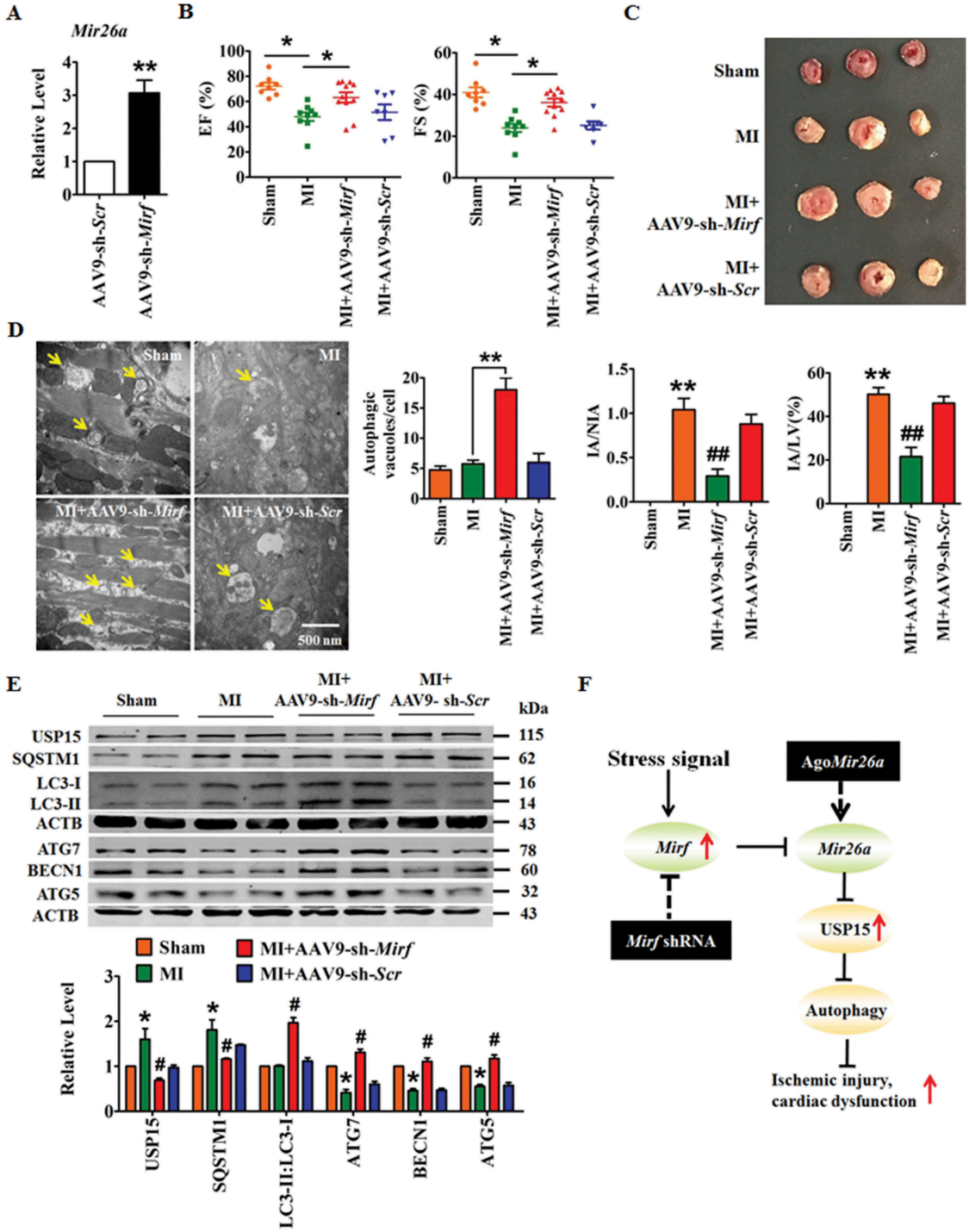

Figure 8. Silencing of *2810403D21Rik/Mirf* alleviates myocardial injury and protects heart function in a mouse model of MI. (A) Upregulation of *Mir26a* in the hearts of WT mice after inhibition of *2810403D21Rik/Mirf*. n = 6. $^{**}p < 0.01$ *vs*. AAV9-sh-*Scr*. AAV9-sh-*Scr*, negative control of AAV9-sh-*2810403D21Rik/Mirf*. Silencing of *2810403D21Rik/Mirf* by AAV9-sh-*2810403D21Rik/Mirf* improved heart function (B) (n = 11. $^{*}p < 0.05$), reduced infarct size (C) (n = 5. $^{**}p < 0.01$ vs. Sham; ##p < 0.01 vs. MI) in MI mice. Transmission electron microscopy (D) (n = 5. $^{**}p < 0.01$) and western blot assay (E) (n = 6. $^{*}p < 0.05$ *vs*. Sham; $^{\#}p < 0.05$ *vs*. MI) show the pro-autophagic effects of *2810403D21Rik/Mirf* inhibition. The yellow arrows point to autophagic vesicles. AAV9-sh-*Scr*, negative control of AAV9-sh-*2810403D21Rik/Mirf*. (F) Proposed autophagic signaling mechanism for *2810403D21Rik/Mirf* and *Mir26a* during MI. Cardiac stress inhibits expression of *Mir26a* by increasing the expression of *2810403D21Rik/Mirf* and blocks autophagy, resulting in post-transcriptional de-repression of USP15 and leading to ischemic injury and cardiac dysfunction, respectively.

not affect the level of miRNA expression, but our results, as well as other studies investigating interactions between lncRNAs and miRNAs, suggest that lncRNAs not only affect the activity of target miRNAs but also regulate their expression [34,35]. It is not likely that ceRNA regulation is the only mechanism by which lncRNAs affect levels of miRNAs. We concluded that lncRNA *2810403D21Rik/Mirf* regulated *Mir26a* only partially through ceRNA, but the other mechanisms of *Mir26a* inhibition by *2810403D21Rik/Mirf* need to be studied further.

USP15 is a member of a family of deubiquitinating enzymes, which are shown to inhibit mitochondrial autophagy by the activation of PINK1/PRKN pathway [36]. PINK1 can be rapidly degraded by proteolytic enzymes in healthy mitochondria but the proteolytic enzyme responsible for PINK1 degradation is inhibited in injured mitochondria, leading PINK1 to gather on damaged mitochondria and recruit PRKN (parkin RBR E3 ubiquitin protein ligase) from the cytoplasm into the mitochondria. The resulting increased E3 ubiquitin ligase activity induces the ubiquitination of mitochondrial matrix proteins, which leads to accumulation of SQSTM1 in the mitochondrial matrix. SQSTM1 combines with LC3 to initiate autophagy. It has been confirmed that mammalian MFN (mitochondrial fusion proteins) 1 and 2, and the VDAC1 (voltage-dependent anion channel protein 1) are substrates for ubiquitination by PRKN. PRKN degrades MFN1 and MFN2 by ubiquitination and further inhibits the fusion of damaged and healthy mitochondria, activating mitochondrial autophagy to remove damaged mitochondria. Some deubiquitinating enzymes, such as USP8, USP15, and USP30, can remove the ubiquitin chain from PRKN or its substrate, thereby inhibiting the occurrence of mitochondrial autophagy [17,37,38]. USP15 has been reported to antagonize mitophagy, a subtype of autophagy, in fibroblasts in patients [17]. The present study found that *Usp15* was a potential target of *Mir26a* and mediated the pro-autophagic and cardioprotective effects of *Mir26a* against ischemic injury.

Generally, the expression level lncRNAs is much lower in tissues [39], but the biological functions of lncRNAs are not limited by their low expression. We found that *2810403D21Rik/Mirf* regulated expression of *Mir26a* and overexpression of *2810403D21Rik/Mirf* increased the level of USP15, likely due to repression of *Mir26a*. *2810403D21Rik/Mirf* suppressed the autophagy in cardiomyocytes and knockdown of *2810403D21Rik/Mirf* protected the heart and cardiomyocytes against cardiac injury by enhancing autophagy under both *in vivo* MI and *in vitro* H_2O_2 conditions. The present study focused mainly upstream, on *Mir26a* modulation of cardiac autophagy and the interactions between *2810403D21Rik/Mirf* and *Mir26a*. Downstream, we have shown that *Mir26a* may activate autophagy by targeting *Usp15*, since USP15 can inhibit mitophagy. This mechanism will be studied in future work.

In short, the present work identified a novel anti-autophagic lncRNA, *2810403D21Rik/Mirf*, which exaggerated ischemic cardiac injury by modulating *Mir26a* levels via ceRNA regulation. Thus, adjusting expression of *2810403D21Rik/Mirf* may provide a novel approach for prevention and treatment of AMI.

Materials and methods

Animal treatment

Male C57BL/6 mice weighing 20–30 g were purchased from Beijing Vital River Laboratory Animal Technology Co., Ltd. (Beijing, China). Cholesterol-conjugated *Mir26a* mimic (ago*Mir26a*) (RiboBio Company, Ltd., Guangzhou, China) was injected through tail-vein at a dosage of 80 mg/kg/d in 0.2 ml saline once a day for three consecutive days, followed by creation of a mouse MI model on day 4. To evaluate the role of *2810403D21Rik/Mirf* in MI, adeno-associated virus 9 carrying the *2810403D21Rik/Mirf* shRNA (AAV9-sh*-2810403D21Rik/Mirf*) (Biowit Technology, Shenzhen, China) or its scramble control construct (AAV9-sh-*Scramble*) was injected once through tail-vein at a dosage of 1x10^11 vg per mice followed by creation of a mouse MI model after two weeks.

To establish an MI model, mice were anesthetized with sodium pentobarbitone (40 mg/kg, i.p.) and xylazine (12.5 mg/kg, i.p.). And placed in the supine position with the upper limbs taped to the table. A 1–1.5 cm incision was made along the left side of the sternum. The muscle layers of the chest wall were bluntly dissected to avoid bleeding. The thorax was opened at the point of the most pronounced cardiac pulsation and the right side of the chest was pressed to push the heart out of the thoracic cavity. The left anterior descending coronary artery was occluded and then the chest was closed. All surgical procedures were performed under sterile conditions. After 24 h, mice were anesthetized with sodium pentobarbitone (40 mg/kg, i.p.) and xylazine (12.5 mg/kg, i.p.) and sacrificed with their hearts quickly isolated. The animals in the sham control group underwent open chest procedures without coronary artery occlusion. The procedures were in accordance with the regulations of the Ethics Committee of Harbin Medical University and the Guide for the Care and conformed to the Guide for the Care and Use of Laboratory Animals published by the US National Institutes of Health (NIH Publication No. 85–23, 2011).

Generation of Mir26a knockdown mice

The fragment of Spong-*Mir26a* (gtcgacgaattcagcctatccttcgtacttgaagcacagcctatccttcgtacttgaagcacagcctatccttcgtacttgaagcacagcctatccttcgtacttgaagcacagcctatccttcgtacttgaagcacagcctatccttcgtacttgaagcacaagcttgaattc) was synthesized by Shanghai Biological Engineering Inc. The fragment was subcloned into the *Sal*I (R4054) and *Hind*III (R4044) sites of Bluescript vector (Huayueyang Biotechnology, Beijing, VECT4840) carrying the cardiac-specific *Myh6/αMHC* promoter and human GH (growth hormone) poly(A)$^+$ signal, and then injected into fertilized eggs of BL6/SJL hybrid mice using the pronuclear injection method. Founder mice were then back-crossed with C57/BL6 mice many times to obtain a clean background.

TTC staining

We collected the heart at 24 h after myocardial infarction, and the hearts were washed by cold PBS (Beyotime, C0221A) to drain residual blood. The hearts were cut into 5–6 sections with the same thickness, then soaked in 1% TTC dyeing buffer (Solarbio, G3005), and incubated for 20 min at 37°C. The sections were fixed with 4% paraformaldehyde for 30 min after staining uniformly and take photos for the sections placing in order. And the infarcted area was calculated by ImageJ (NIH).

Echocardiograph

Mice were anesthetized using 4–5% isoflurane (Sigma, T48402)-inhalation anesthesia. Cardiac hemodynamics was analyzed using ultrasound with a Vevo2100 system (VisualSonics, Toronto, Canada) 24 h after MI. Mice were anesthetized and left ventricular function was assessed two-dimensional M-mode recording using a 30 MHZ transducer with continuous oxygen supply. Functional parameters were evaluated including fractional shortening (FS) and ejection fraction (EF).

Cell culture and treatment

Neonatal mice cardiomyocytes (NMCMs) were prepared by the following procedures: 1- to 3-d-old C57BL/6 mouse were anesthetized using 4–5% isoflurane-inhalation anesthesia. Mouse hearts were finely minced and placed together in 0.25% trypsin (Thermofisher, 25200056); 5-bromo-2-deoxyuridine (BrdU; Solarbio, B8010) was added at 0.1 mM to eliminate the cardiac fibroblasts. Dispersed NMCMs were cultured in Dulbecco's modified Eagle's medium (DMEM; Biological Industries, 01–052-1-A) containing 10% fetal bovine serum (Biological Industries, 04–001-1C) in a 5% CO_2 and 37°C humidified atmosphere. The cells were seeded in 6-well plates, cultured for 48 h and transfected with 100 nM *Mir26a* or *AMO-26a*, with X-treme GENE siRNA transfection reagent (Roche, 06366244 001). Forty-eight h after transfection, cells were used for total protein purification. 3-methyladenine (3-MA; 5 mM), an antagonist of autophagy, purchased from Sigma-Aldrich (M9281) was dissolved in the culture medium.

MTT assay

MTT assay was used to determine cell viability. NMCMs were plated in 96-well culture plates. After 48 h of transfection, the cells were incubated with 20 μl MTT (Sigma, M2128) (0.5 mg/ml) and 180 μl DMEM for 4 h. The culture medium was carefully removed and 150 μl DMSO was added to each well to dissolve the formazan. After rocking for 15 mins at room temperature, the absorbance values were read at 490 nm using an Infinite®200PRO microplate spectrophotometer (Tecan, Salzburg, Austria).

Luciferase assay

Usp15 3′-UTR containing the conserved *Mir26a* binding sites and mutated 3′-UTRs were synthesized by Invitrogen (Carlsbad, CA, USA). The fragment was subcloned into the SacI and HindIII sites downstream of the luciferase gene in the pMIR Reporter (Addgene, MLCC13738). HEK293 cells (American Type Culture Collection, ATCC#1531) were cultured in DMEM containing 10% fetal bovine serum and 1% penicillin/streptomycin. HEK293 cells were co-transfected in 24-well plates with WT *Usp15* or mutant constructs and *Mir26a*, negative control or *AMO-26a*. The *Mir26a* sensor reporter was constructed according to the method previously described [35]. Briefly, the mouse genomic sequence (200 bp) flanking pre-*Mir26a* was inserted into the pGL3 vector (Promega, E1761) in reverse orientation downstream of the luciferase gene coding region. NMCMs were co-transfected with *Mir26a* sensor and si-*Mirf*/*Mirf*/*Mir26a* or their negative control using the Lipofectamine 2000 reagent (Invitrogen,11668019). After 48 h of transfection, the cells were harvested and lysed. Luciferase activity was assayed using the Dual Luciferase Reporter Assay System (Promega, E1910) according to the manufacturer's instructions. Firefly luciferase values were normalized to Renilla, and relative ratios of Firefly to Renilla activity was reported.

Quantitative real-time PCR (qRT-PCR)

Total RNA was isolated from heart tissues or cultured NMCMs using a Trizol standard protocol. The integrity, quantity, and purity of RNA were examined using NanoDrop 8000 Spectrophotometer (Thermo Scientific, Wilmington, USA). For each sample, 500 ng of total RNA was converted to cDNA using High Capacity cDNA Reverse Transcription Kit (Transgene, AT341-02). The relative expression levels of mRNAs and miRNAs were quantified by qRT-PCR with SYBR Green I (Roche, 4913914001). Threshold cycle (Ct) was determined and relative mRNA and miRNA levels were calculated based on the Ct values and normalized to *Actb* or *Rnu6* in each sample. And the primers are shown in Table 1.

Western blot

For western blot analysis, total protein samples were extracted from tissues or cells. Briefly, tissues or cells were lysed with RIPA lysis buffer (Beyotime, P0013K) containing a complete protease inhibitor cocktail (Roche, 04963159001). Protein samples (60 μg) were fractionated on a 10% or 12% SDS-PAGE. After electrophoretic transfer to a Pure Nitrocellulose Blotting membrane (Pall Life Science, 66485), the blots were probed with primary antibodies and ACTB/β-actin (Proteintech, 60008–1-Ig) as an

Table 1. The primers in RT-qPCR assays.

Primers	Sequence(5′-3′)
RNU6 RT	CGCTTCACGAATTTGCGTGTCAT
Mir26a RT	GTCGTATCCAGTGCGTGTCGTGGAGTCGGCAATTGCACTGGATACGACAGCCTAT
Rnu6-F	CGCTTCACGAATTTGCGTGTCAT
Rnu6-R	GCTTCGGCACATATACTAAAAT
Mm-*Mir26a*-F	GCGTAGCAGCGGGAACAGT
Mm-*Mir26a*-R	CCAGTGCGTGTCGTGGAGT
Mm-*Mirf*-F	TCTTTCCCAGTTCTCCTTGG
Mm-*Mirf*-R	GCAGTAGCAAATTCCCCAAA
Mm-*Usp15*-F	CCGTGGATGAAACCTGAGT
Mm-*Usp15*-R	TGAAGAGCCAGTGTGGTGAG

internal control. Primary antibodies against USP15 was purchased from Proteintech (14354–1-AP), antibodies against ATG5 (2630s) and ATG7 (8558s) were obtained from Cell Signaling Technology, and antibodies against BECN1 (057k4822), LC3B (L7543) and SQSTM1 (103M4785V) were obtained from Sigma-Aldrich. The immunoreactivity was detected using Odyssey Infrared Imaging System (Gene Company Limited, Hongkong, China). The bands were quantified by measuring the band density.

Confocal imaging

As previously described [6], NMCMs transfected with tandem GFP-mRFP-LC3 were examined by laser microscopy. The number of GFP and mRFP puncta per cell was manually quantified. At least 10 cells in each of three independent experiments were randomly analyzed.

Transmission electron microscopy

Left ventricular tissues were sliced into ultrathin sections. These sections were fixed with 4% paraformaldehyde and 1% glutaraldehyde in PBS at 4°C overnight. The preparations were washed and dehydrated with increasing concentrations of ethanol, followed by embedding and sectioning. The cardiac slices were examined by a microscopist under an H7650 transmission electron microscope (Hitachi, Japan). For each treatment, the micrographs of at least 15 unique cells were recorded.

Affinity-isolation assay with biotinylated miRNA

Cardiomyocytes were transfected with biotinylated miRNA (50 nM), harvested 48 h after transfection. The cells were washed with PBS and briefly vortexed then incubated in a lysis buffer (20 mM Tris, pH 7.5, 200 mM NaCl, 2.5 mM $MgCl_2$, 0.05% Igepal (Sigma, I8896), 60 U/ml Superase-In (Ambion, CA, USA), 1 mM DTT, protease inhibitors (Roche, 04963159001) on ice for 10 min. The lysates were pre-cleared by centrifugation and 50 ml of the samples were aliquoted for input. The remaining lysates were incubated with M-280 streptavidin magnetic beads (Invitrogen, 14203). To prevent nonspecific binding of RNA and protein complexes, the beads were coated with RNase-free bovine serum albumin (Sigma-Aldrich, C3023) and yeast tRNA (Invitrogen, 15401029). The beads were incubated at 4°C for 3 h, washed twice with ice-cold lysis buffer, then three times with the low salt buffer (0.1% SDS, 1% Triton X-100 (Thermofisher, HFH10), 2 mM EDTA, 20 mM Tris-HCl, pH 8.0, 150 mM NaCl), and once with the high salt buffer (0.1% SDS, 1% Triton X-100, 2 mM EDTA, 20 mM Tris-HCl, pH 8.0, 500 mM NaCl). The bound RNAs were purified for qRT-PCR using Trizol (Invitrogen, 15596–026). *Mir26a* affinity-isolation probe, 5′- UUCAAGUAAUCCAGGAUAGGCU-3′, and NC affinity-isolation probe, 5′- UUUGUACUACACAAAAGUACUG- 3′.

RNA affinity-isolation assay with biotinylated DNA probe

The biotinylated DNA probe complementary to *2810403D21Rik/Mirf* was synthesized and dissolved in 500 ml of wash/binding buffer (0.5 M NaCl, 20 mM Tris-HCl, pH 7.5, 1 mM EDTA). The probes were incubated with streptavidin-coated magnetic beads (Pierce, 88816) at 25°C for 2 h to generate probe-coated magnetic beads. Cardiomyocyte lysates were incubated with probe-coated beads, and, after washing with the wash/binding buffer, the RNA complexes bound to the beads were eluted and extracted for qRT-PCR analysis. *2810403D21Rik/Mirf* affinity-isolation probe, 5′-TTCCTGTAAGGGCAATCGGACCCTTTCCGGTGAGGGAACCTCTCTCCAGACATGATCAAGAGAAACTGGCGAGGGACTGACATGATCTAGCTTACCTTGGGTCACCGAACGGATTTGGCATGTGACATAATTATCCCAGCGATCACTAAAACTGTAAATTTGGATGCAATTAAGAGAGAAAACTCCACACATTTATGGAAATTTAAGATTTGCAGCTTGCTGGCTTGCTGAGTGGAAAATGATTCTTTCCCAGTTCTCCTTGGTTTCTTCCTTTCATGAATTGATTAACACTGAGAGATTATGTTTTAATTATGTCGACTAGAGGTTTTAAATGATTCTAGGTTTCTGTGTCCATTTGTTTTCCTAGGTTTGGGGAATTTGCTACTGCAATATCGTTGTATAGATATTCTTTGCTTTAGTGAGAAACTCAGCTCCTTCTACTCTGTGGTTCTTAGCTTTAGTCTATTGTACACATCACAGAGTTAATGAAAGCTGTGGTCATACTTGATTTTTTCTTCATTACTATTGAAATAAAGCATATCCTTG −3′, and Scramble affinity-isolation probe, 5′- CTTGGTACCGAGCTCGGATCCACTAGTCCAGTGTGGTGGAATTCTGCAGATATCCAGCACAGTGGCGGCCG-3′.

Statistical analysis

All the data were expressed as the mean±SEM. GraphPad Prism 5.0 was used for our statistical analysis. For two group comparisons, Student *t*-test was used. For multiple group comparisons, one-way ANOVA was used with Bonferroni post-test for comparisons between selected two groups as well as Dunnett post-test for comparisons among all other treatment groups to the corresponding control. A value $p < 0.05$ was considered statistically significant.

Disclosure statement

No potential conflict of interest was reported by the authors.

Funding

This study was supported by the National Natural Science Foundation of China (81770284, 31671187, 81673425).

ORCID

Xuelian Li http://orcid.org/0000-0001-9043-8580

References

[1] Qian L, Van Laake LW, Huang Y, et al. miR-24 inhibits apoptosis and represses Bim in mouse cardiomyocytes. J Exp Med. 2011;208:549–560.
[2] Orogo AM, Gustafsson AB. Cell death in the myocardium: my heart won't go on. IUBMB Life. 2013;65:651–656.
[3] Shirakabe A, Zhai P, Ikeda Y, et al. Drp1-dependent mitochondrial autophagy plays a protective role against pressure

overload-induced mitochondrial dysfunction and heart failure. Circulation. 2016;133:1249–1263.
[4] Qin Q, Qu C, Niu T, et al. Nrf2-mediated cardiac maladaptive remodeling and dysfunction in a setting of autophagy insufficiency. Hypertension. 2016;67:107–117.
[5] Nishida K, Yamaguchi O, Otsu K. Crosstalk between autophagy and apoptosis in heart disease. Circ Res. 2008;103:343–351.
[6] He H, Liu X, Lv L, et al. Calcineurin suppresses AMPK-dependent cytoprotective autophagy in cardiomyocytes under oxidative stress. Cell Death Dis. 2014;5:e997.
[7] Cai B, Ma W, Bi C, et al. Long noncoding RNA H19 mediates melatonin inhibition of premature senescence of c-kit(+) cardiac progenitor cells by promoting miR-675. J Pineal Res. 2016;61:82–95.
[8] Liang H, Zhang C, Ban T, et al. A novel reciprocal loop between microRNA-21 and TGFbetaRIII is involved in cardiac fibrosis. Int J Biochem Cell Biol. 2012;44:2152–2160.
[9] Yang B, Lin H, Xiao J, et al. The muscle-specific microRNA miR-1 regulates cardiac arrhythmogenic potential by targeting GJA1 and KCNJ2. Nat Med. 2007;13:486–491.
[10] Luo X, Pan Z, Shan H, et al. MicroRNA-26 governs profibrillatory inward-rectifier potassium current changes in atrial fibrillation. J Clin Invest. 2013;123:1939–1951.
[11] Liu Y, Wang Z, Xiao W. MicroRNA-26a protects against cardiac hypertrophy via inhibiting GATA4 in rat model and cultured cardiomyocytes. Mol Med Rep. 2016;14:2860–2866.
[12] Zhang Y, Qin W, Zhang L, et al. MicroRNA-26a prevents endothelial cell apoptosis by directly targeting TRPC6 in the setting of atherosclerosis. Sci Rep. 2015;5:9401.
[13] Huang ZP, Ding Y, Chen J, et al. Long non-coding RNAs link extracellular matrix gene expression to ischemic cardiomyopathy. Cardiovasc Res. 2016;112(2):543–554.
[14] Wang K, Liu F, Liu CY, et al. The long noncoding RNA NRF regulates programmed necrosis and myocardial injury during ischemia and reperfusion by targeting miR-873. Cell Death Differ. 2016;23:1394–1405.
[15] Zhang X, Sha M, Yao Y, et al. Increased B-type-natriuretic peptide promotes myocardial cell apoptosis via the B-type-natriuretic peptide/long non-coding RNA LSINCT5/caspase-1/interleukin 1beta signaling pathway. Mol Med Rep. 2015;12:6761–6767.
[16] Boon RA, Jae N, Holdt L, et al. Long noncoding RNAs: from clinical genetics to therapeutic targets? J Am Coll Cardiol. 2016;67:1214–1226.
[17] Cornelissen T, Haddad D, Wauters F, et al. The deubiquitinase USP15 antagonizes Parkin-mediated mitochondrial ubiquitination and mitophagy. Hum Mol Genet. 2014;23:5227–5242.
[18] Salmena L, Poliseno L, Tay Y, et al. A ceRNA hypothesis: the Rosetta Stone of a hidden RNA language? Cell. 2011;146:353–358.
[19] Liu J, Li Y, Lin B, et al. HBL1 is a human long noncoding RNA that modulates cardiomyocyte development from pluripotent stem cells by counteracting MIR1. Dev Cell. 2017;42:333–48 e5.
[20] Ounzain S, Crippa S, Pedrazzini T. Small and long non-coding RNAs in cardiac homeostasis and regeneration. Biochim Biophys Acta. 2013;1833:923–933.
[21] Barwari T, Joshi A, Mayr M. MicroRNAs in cardiovascular disease. J Am Coll Cardiol. 2016;68:2577–2584.
[22] Harada M, Luo X, Qi XY, et al. Transient receptor potential canonical-3 channel-dependent fibroblast regulation in atrial fibrillation. Circulation. 2012;126:2051–2064.
[23] Doria A, Gatto M, Punzi L. Autophagy in human health and disease. N Engl J Med. 2013;368:1845.
[24] Taneike M, Yamaguchi O, Nakai A, et al. Inhibition of autophagy in the heart induces age-related cardiomyopathy. Autophagy. 2010;6:600–606.
[25] Huangfu L, Liang H, Wang G, et al. miR-183 regulates autophagy and apoptosis in colorectal cancer through targeting of UVRAG. Oncotarget. 2016;7:4735–4745.
[26] Zhu H, Tannous P, Johnstone JL, et al. Cardiac autophagy is a maladaptive response to hemodynamic stress. J Clin Invest. 2007;117:1782–1793.
[27] Gottlieb RA, Mentzer RM. Autophagy during cardiac stress: joys and frustrations of autophagy. Annu Rev Physiol. 2010;72:45–59.
[28] Zhang J, He Z, Xiao W, et al. Overexpression of BAG3 attenuates hypoxia-induced cardiomyocyte apoptosis by inducing autophagy. Cell Physiol Biochem. 2016;39:491–500.
[29] Su M, Wang J, Wang C, et al. MicroRNA-221 inhibits autophagy and promotes heart failure by modulating the p27/CDK2/mTOR axis. Cell Death Differ. 2015;22:986–999.
[30] Thum T, Condorelli G. Long noncoding RNAs and microRNAs in cardiovascular pathophysiology. Circ Res. 2015;116:751–762.
[31] Viereck J, Kumarswamy R, Foinquinos A, et al. Long noncoding RNA Chast promotes cardiac remodeling. Sci Transl Med. 2016;8:326ra22.
[32] Wang Z, Zhang XJ, Ji YX, et al. The long noncoding RNA Chaer defines an epigenetic checkpoint in cardiac hypertrophy. Nat Med. 2016;22:1131–1139.
[33] Lu W, Huang SY, Su L, et al. Long noncoding RNA LOC100129973 suppresses apoptosis by targeting miR-4707-5p and miR-4767 in vascular endothelial cells. Sci Rep. 2016;6:21620.
[34] Zhao X, Sun J, Chen Y, et al. lncRNA PFAR promotes lung fibroblast activation and fibrosis by targeting miR-138 to regulate the YAP1-twist axis. Mol Ther. 2018;26:2206–2217.
[35] Liang H, Pan Z, Zhao X, et al. LncRNA PFL contributes to cardiac fibrosis by acting as a competing endogenous RNA of let-7d. Theranostics. 2018;8:1180–1194.
[36] Wang Y, Serricchio M, Jauregui M, et al. Deubiquitinating enzymes regulate PARK2-mediated mitophagy. Autophagy. 2015;11:595–606.
[37] Durcan TM, Tang MY, Perusse JR, et al. USP8 regulates mitophagy by removing K6-linked ubiquitin conjugates from parkin. Embo J. 2014;33:2473–2491.
[38] Bingol B, Tea JS, Phu L, et al. The mitochondrial deubiquitinase USP30 opposes parkin-mediated mitophagy. Nature. 2014;510:370–375.
[39] Wang K, Liu CY, Zhou LY, et al. APF lncRNA regulates autophagy and myocardial infarction by targeting miR-188-3p. Nat Commun. 2015;6:6779.